PAPER 66 (SESSION V)

The effect of intermetallic particles on fatigue crack propagation in aluminium alloys

D. BROEK,

Senior research scientist, National Aerospace Laboratory N.L.R. Sloterweg 145, Amsterdam, The Netherlands.

Summary

Electron fractography of fatigue in aluminium alloys has shown that intermetallic particles and inclusions have no significant effect on the crack growth when stress levels crack propagation rates are low. In such cases crack growth usually occurs along the interface between the particle and the matrix.

At higher stress levels intermetallic particles induce small amounts of ductile tearing and therefore increase the crack growth rate. This explains experimentally observed deviations from Paris' crack propagation law.

Some other features of the fracture surfaces which are of use in service failure analysis are briefly discussed and explained.

Introduction

Although Grosskreutz and Shaw [1] have shown that inclusions and intermetallic constituents play a role in the initiation of fatigue cracks, information about the effect of intermetallic particles on the propagation of the cracks is still very limited. There is some evidence that inclusions have an influence on static fracture, e.g. Birkle *et al.*[2] have found a correlation between the fracture toughness of steel and the amount of sulphide and carbide inclusions. Broek [3] examined the plane stress fracture toughness of Al-Cu alloys of nominally the same nominal composition, but obtained from different manufacturers. A vague correlation was found between toughness and the amount of intermetallic constituents. In an earlier investigation Schijve [4] compared the fatigue crack propagation rates in the same materials. Although there were significant differences in growth rates, there was no correlation with size or distribution of particles.

The present paper gives the results of an extensive investigation into the effect of intermetallic particles on fatigue crack growth in aluminium alloys using electron fractography.

Inclusions and fatigue crack propagation rate

Electron fractography showed that the effect of inclusions depends upon the crack propagation rate. At low crack growth they have little influence as is shown by the following examples.

Fig. 1 shows the effect of a fairly large particle: here the crack front remained straight until it reached the particle, when the particle, at this point, cleaved as is shown by the faint river markings on its fracture

surface. After cleavage of the particle the crack had a locally advanced front, and in its vicinity crack propagation was slowed down as illustrated by the closely spaced striations in front of the particle. The striation spacing at arrow A (Fig. 1) shows that the crack growth rate was increased slightly for a few cycles under the influence of this advanced crack front. The striation spacing at B indicates that the increase of growth rate occurred at a later time on this side of the particle. Although the inclusion clearly affected the local pattern of crack propagation, it is clear that the overall crack growth rate was not appreciably affected. The consistent striation spacings in Fig. 1 also shows that the many small particles (small arrows) had no effect on crack propagation. These small particles were apparently pulled out of the matrix.

Another example of a cleaved particle is shown in Fig. 2. In this case secondary cracks were initiated along the sides of the particle and bowed outward (curved arrows) to link up with the main front. Secondary cracks initiated at the small particles are shown in Fig. 3; these had no marked effect on the crack growth rate.

Figs. 3, 4 and 5 show examples where the fatigue crack has propagated along the interface between the particle and the matrix. Optical micrographs of cross sections through fatigue cracks grown at similar rates are shown in Fig. 6 and these confirm that in almost all cases the crack passed along the interface between the matrix and the intermetallic constituents (A), the smaller particles were pulled out of the matrix (B). Some particles in the crack path (C) as well as several in the vicinity of the crack path (D) cleaved, although these did not initiate secondary cracks.

Fig. 7 is a fractograph of a programme fatigue test, specimen and shows the effect of a row of particles; the crack propagated along the interface between the particle and the matrix. At 'A' crack growth was increased locally, while at 'B' the crack trailed slightly behind the main front.

The general conclusion is that at low crack propagation rates the crack passes round rather than through intermetallic particles and that such particles only slightly affect the fatigue crack growth rate.

The situation is different at higher crack propagation rates (in the order of 1 micron per cycle and more). This is shown by Figs. 8 and 9, which are similar to fractographs presented previously by Pelloux [5]. High growth rates are a result of a high stress intensity at the crack tip (large crack or high loads). Due to the higher stresses and strains, particles in front of the crack tip may cleave or lose coherency with the matrix, thus initiating a void. The remaining material between the void and the crack tip now may rupture by ductile tearing, thus inducing a local jump of the crack front. This is shown by the areas with dimples in Figs. 8 and 9,

which are evidence of a mechanism of void coalescence during ductile rupture.

At these higher propagation rates the effect of inclusions cannot be neglected. Comparison of the crack growth rate measured during the test with striation spacing reveals a large discrepancy caused by small amounts of static fracture. At still higher crack rates striations become very rare and the fracture surface consists primarily of dimples. On the basis of Figs. 8 and 9 one may conclude that the crack growth rate would have been much smaller in the absence of inclusions. Neglecting inclusions the 'true fatigue' growth rate (by striation formation) would have been about 0·3 microns per cycle in Fig. 8, instead of 1 micron per cycle actually observed in the test.

Crack propagation rate and stress intensity factor

True fatigue crack propagation in aluminium alloys is considered to be by a mechanism of striation formation. Programme fatigue tests have indicated that the crack propagates during each cycle by the formation of one striation (see Fig. 7). This suggests that the striation spacing should equal the growth rate per cycle. Many investigators [6], [7], [13] have shown the close correlation between striation spacing and observed growth rate. However, in general these observations concerned only a limited range of crack growth rates. On the basis of the present investigation deviations at high growth rates might be expected. This might explain certain discrepancies between test results and proposed crack propagation laws.

The elastic stress field at the tip of a central transverse crack in a tensile specimen can be fully described by one single parameter $K = S\sqrt{(l)}$ (stress intensity factor), where S is the stress at the specimen ends and l is the semi crack length [8]. Paris *et al.*[8] were the first to suggest that as K fully describes the stresses at the crack tip it should also describe what occurs at the crack tip. In other words the fatigue crack propagation rate should be some function of K. Many workers have proposed a simple power law: $dl/dn = C.K^n$, where dl/dn is the growth rate per cycle, C and n are constants.

It was therefore decided to check the correlation between growth rate and striation spacing over a large range of propagation rates. For this purpose 8 specimens were prepared, four of an aluminium-zinc alloy (7075-T6) and four of an aluminium-copper alloy (2024-T3). A sharp central notch was machined in each specimen and they were cycled at various stress levels having a cycle ratio $R = 0{\cdot}05$. Crack growth was recorded by using a low power binocular microscope and stroboscopic light.

The observed crack growth rates are plotted in Fig. 10 as a function of the maximum stress intensity factor during the cycle (corrected for finite

width using the Irwin [9] correction factor). The results confirm that, for a certain value of the cycle ratio R, data of tests with different amplitudes fall on a single curve, and show that the crack propagation rate is controlled by the stress intensity factor. For other values of the cycle ratio parallel curves have been obtained [10]. However, on this double-log plot the data produce an S-shaped curve instead of the straight line required for a simple power law.

Replicas for electron fractography were taken from whole fracture surface of all eight specimens and over 200 micrographs were examined. Striation spacing was measured as the average spacing of 5 or 10 successive striations at all suitable places. The striation spacing has been plotted in Fig. 11 against the stress intensity factor. Each data point in this figure is the average of all measurements made on one micrograph.

This figure once more confirms that in general a striation is formed during each cycle. Furthermore the data indicate that the simple power relation between growth rate and stress intensity factor need not be unrealistic. The relation breaks down at high crack rates, where there is almost no true fatigue crack propagation. If striations are formed in this region their spacing is smaller than the overall growth rate, as discussed in the previous section.

At low crack growth rates the deviations from a straight line are smaller in Fig. 11 than in Fig. 10. This can be explained by assuming that crack propagation does not take place over the whole crack front in every cycle, as proposed by Schijve [11] and by McMillan and Hertzberg [12] whereas Hoeppner *et al.* [13] state that the correlation between growth rate and spacing of striations does not break down, but that the limited resolution of replicas prevents one from finding striations spaced more closely than say 200 Ångstroms. In the present investigation the smallest spacing observed was 140 Ångstroms, which is about 50 lattice vectors. Striation formation is a result of slip plane decohesion during opening and closing of the crack [14], [15]. It is our opinion that slip plane decohesion of much less than 50 lattice vectors could not produce the complicated topography of a striation over some length and consistently during each cycle. It is felt that this stage must still be considered the crack initiation stage. In the propagation stage striations of a certain minimum size are probably found.

If true fatigue crack propagation is considered to occur as a striation mechanism the power relationship between K and dl/dn is probably applicable. Break down of this relation at high growth rates is the result of static tearing rather than fatigue. Break down at low rates is due to the fact that the crack is still primarily in the initiation stage.

Other effects of hard particles

Features frequently observed in fractographs are tyre tracks (Fig. 12), so called because they resemble the tread marks of an automobile tyre. The present investigation revealed that there are two types of tyre tracks, which will be denoted here as types I and II. Tyre tracks are a secondary result of the presence of inclusions and intermetallic particles.

An explanation for type I (Fig. 12) has been given by Beachem [16], who proposed a mechanism amplified here in Fig. 13. A hard particle torn out of the matrix will make indentations in the mating surface, as the two surfaces are offset during opening and closing of the crack. Elegant micrographs of mating surfaces published by Beachem [16] present an excellent proof of this mechanism. Another example of type I tyre tracks is given here in Fig. 14.

Type II tyre tracks were observed more frequently. Examples are given in Figs. 15, 16 and 17. Ansell *et al.* [17] consider them to be hydrogen precipitation sites, formed in the highly stressed crack tip region. If this were so type II tyre tracks would represent a row of voids and one might expect them to consist of more or less circular marks, which is obviously untrue.

Type II tyre tracks can be better explained as the result of loose hard particles moving across the fracture surface by a 'slip-stick' mechanism. The best evidence for this mechanism is given in Fig. 17. Since there are no discontinuities it is obvious that the short scratches obviously were all formed in one cycle. The tyre tracks are of the same width as the scratches and one scratch ends at a tyre track. The distinction from type I is that a whole row of indentations is formed in one stroke.

It should be emphasized that type II tyre tracks are always accompanied by severe scratching. Which must be a result of rubbing, and they usually occur at high crack growth rates (5 microns per cycle or more). At high crack growth rates one would expect more particles to be completely torn out, such as the one at 'E' in Fig. 6. Also the offset during opening and closing of the crack will be large at high growth rates (large deformations and displacements).

Tyre tracks are only a secondary feature of the fatigue process, but they do show that the deformations at the crack tip must have had a shear component, which was not completely reversed. Tyre tracks are formed during closure of the crack which explains why type II tyre tracks are never observed in static fractures.

Type II tyre tracks are of importance in the analysis of service failures analysis. They occur at high crack growth rates where almost no striations are formed. Thus type II tyre tracks can serve as an identification feature for low cycle fatigue in service failure analysis.

Conclusions

Intermetallic particles and inclusions, although of importance for fatigue crack initiation, have only a slight effect on fatigue crack propagation at low crack growth rates where fracture usually occurs along the interface between the particle and the matrix. However, at higher crack propagation rates these particles do have an effect by inducing small amounts of ductile fracture. This could explain why the power relationship between stress intensity factor and crack growth rate breaks down at high crack propagation rates. In the absence of inclusions the true fatigue crack propagation rate would be much lower. At low crack growth rates deviations from the power law may be due to inhomogeneous crack extension along the crack front.

Two different types of tyre tracks can be observed on fatigue fracture surfaces. They are both caused by hard foreign particles. Type II tyre tracks are a feature typical of low cycle fatigue and as such are of value in service failure analysis.

Acknowledgement

This investigation was sponsored in part by the Department of Scientific Investigations of the Royal Netherlands Air Force.

I am indebted to Mr W. van der Vet for the painstaking microscopy needed to compose Fig. 11.

References

1. GROSSKREUTZ, J. C. and SHAW, G. 'Critical mechanisms in the development of fatigue cracks' (To be published shortly).
2. BIRKLE, A. J., WEI, R. P. and PELLISIER, G. E. 'Analysis of plane strain fracture in steels with different sulfur contents' *A.S.M. Trans.*, vol. 59, p. 981, 1966.
3. BROEK, D. 'Static tests on cracked panels of 2024-T3 alclad sheet materials from different manufacturers' N.L.R. rept. TR-M-2164, 1966.
4. SCHIJVE, J. and DE RIJK, P. 'Fatigue crack propagation in 2024-T3 alclad sheet materials from seven different manufacturers' N.L.R. rept. TR-M-2162, 1966.
5. PELLOUX, R. M. N. 'Fractographic analysis of the influence of constituent particles on fatigue crack propagation in aluminum alloys' *A.S.M. Trans.*, vol. 57, p. 511, 1964.
6. JACOBY, G. 'Observation of crack propagation on the fracture surface' in *Current aeronautical fatigue problems*, Pergamon, 1965.
7. SCHIJVE, J. BROEK, D. and DE RIJK, P. 'The effect of frequency on the crack rate in a light alloy sheet' N.L.R. rept. TN-M-2092, 1961.
8. PARIS, P. C., GOMEZ, M. P. and ANDERSON, W. E. 'A rational analytic theory of fatigue' *The Trend in Engineering*, vol. 13, p. 9, 1961.
9. IRWIN, G. 'Fracture' in *Handbuch der Physik*, Springer Verlag, 1958, p. 551.
10. BROEK, D. and SCHIJVE, J. 'The influence of the mean stress on the propagation of fatigue cracks in aluminium alloy sheet' N.L.R. rept. TR-M-2111, 1963.

11. SCHIJVE, J. 'Analysis of the fatigue phenomenon in aluminium alloys' N.L.R. rept. TR-M-2122, 1964.
12. McMILLAN, J. C. and HERTZBERG, R. W. 'The application of electron fractography to fatigue studies' A.S.T.M. STP 415, 1968.
13. HOEPPNER, D. W. *et al.*, *Fatigue behaviour of materials for the SST; Electron fractographic studies*, Battelle Mem. Inst., Columbus, 1965.
14. BROEK, D. and VAN DER VET, W. 'Systematic electron fractography of fatigue in aluminium alloys' N.L.R. rept. 68002, 1968.
15. SCHIJVE, J. Discussion in A.S.T.M. STP 415, p. 533, 1968.
16. BEACHEM, C. D. 'Microscopic fatigue fracture surface features in 2024-T3 aluminum and the influence of crack propagation angle upon their formation' *A.S.M. Trans.*, vol. 60, p. 324, 1967.
17. ANSELL, G. S. *et al.*, 'Effect of dissolved hydrogen on the fatigue behavior of a SAP-type alloy' *A.S.M. Trans.*, vol. 59, p. 630, 1966.

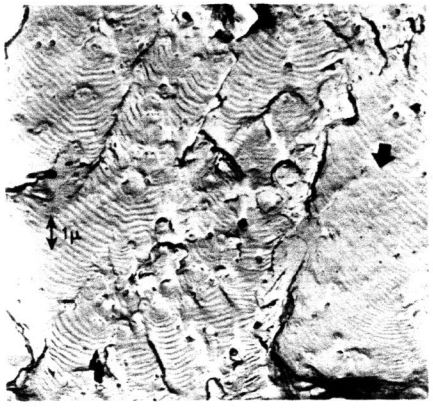

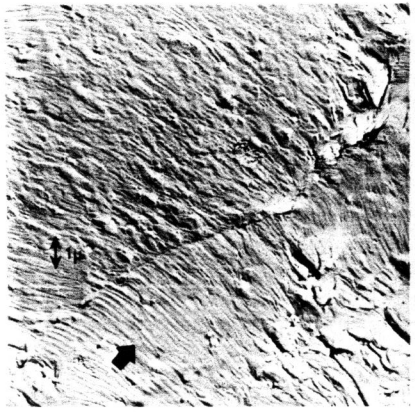

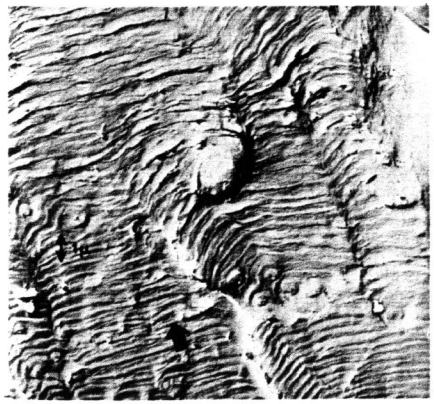

Fig. 1. Effect of large cleaved particle and of small particles on crack growth in 2024-T3. Solid arrow indicates direction of propagation.

Fig. 2. Cracks emanating from cleaved particle, 2024-T3.

Fig. 3. Particles pulled out of matrix, 2024-T3.

Fig. 4. Effect of small particles, 2024-T3.

Fig. 5. Particle pulled out of matrix, 7075-T6.

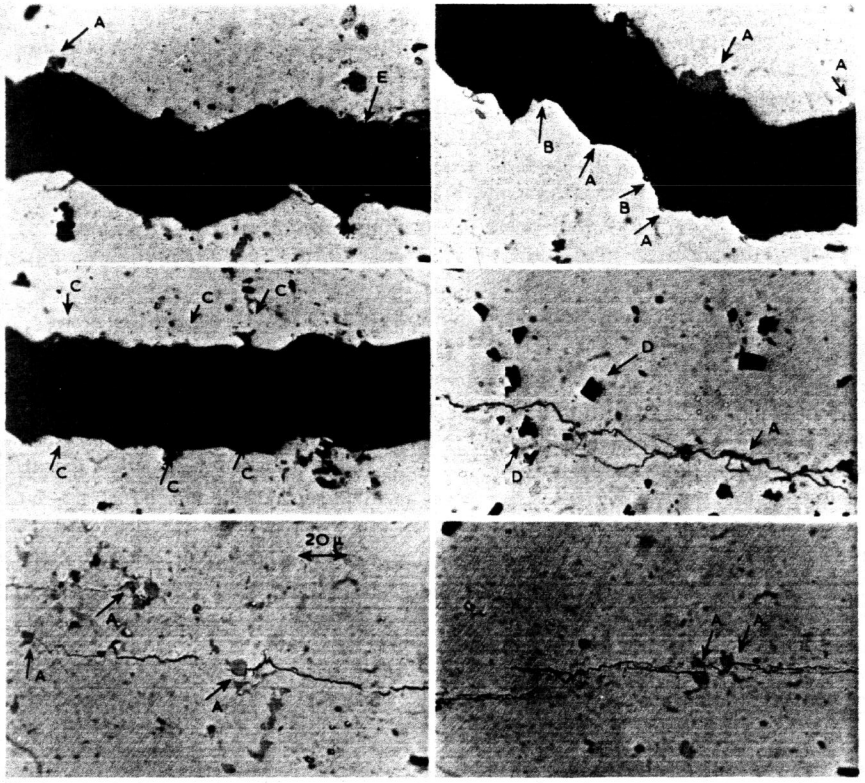

Arrows A: crack along interface; B: particles pulled out of matrix; C: crack through cleaved particles; D: cleaved particles in vicinity of crack path; E: loose particle.
Wide cracks opened up by static tensile load.

Fig. 6. Optical micrographs showing path of fatigue crack along intermetallic particles. 2024-T3.

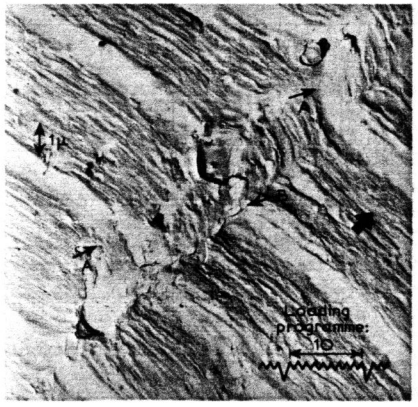

Fig. 7. Effect of row of particles on crack growth in a programme fatigue test 2024-T3.

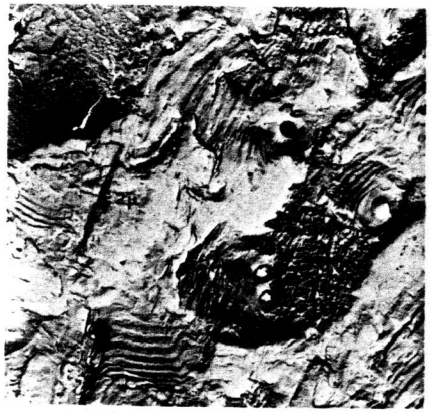

Fig. 8. Static growth due to inclusions at fatigue crack growth rate of 1 micron per cycle in 2024-T3.

Fig. 9. Static growth at inclusions in 7075-T6 at fatigue crack growth rate of 1 micron per cycle.

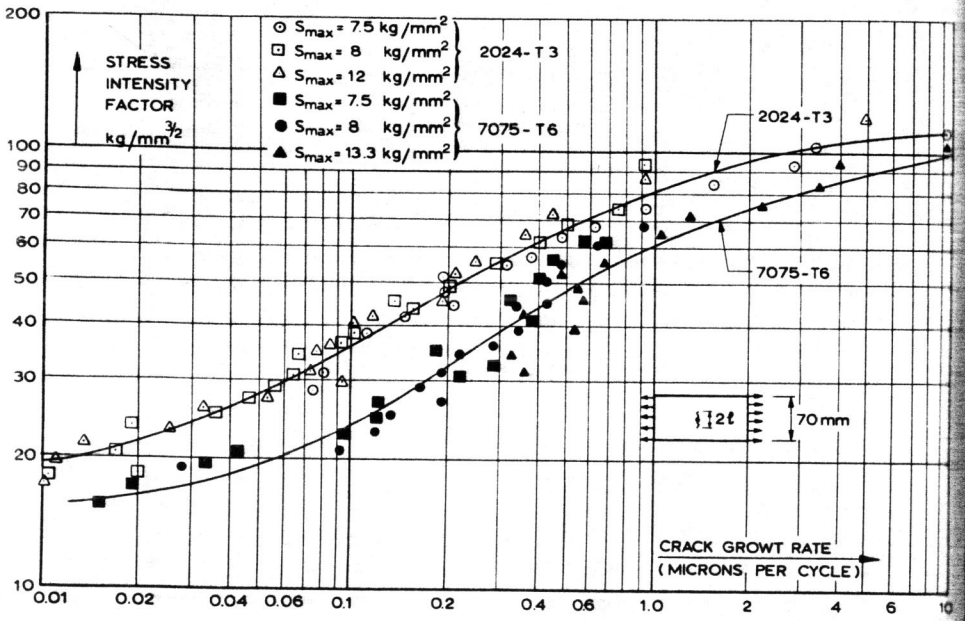

Fig. 10. Relation between stress intensity factor (K_{max}) and crack rate, cycle ratio R = 0·05.

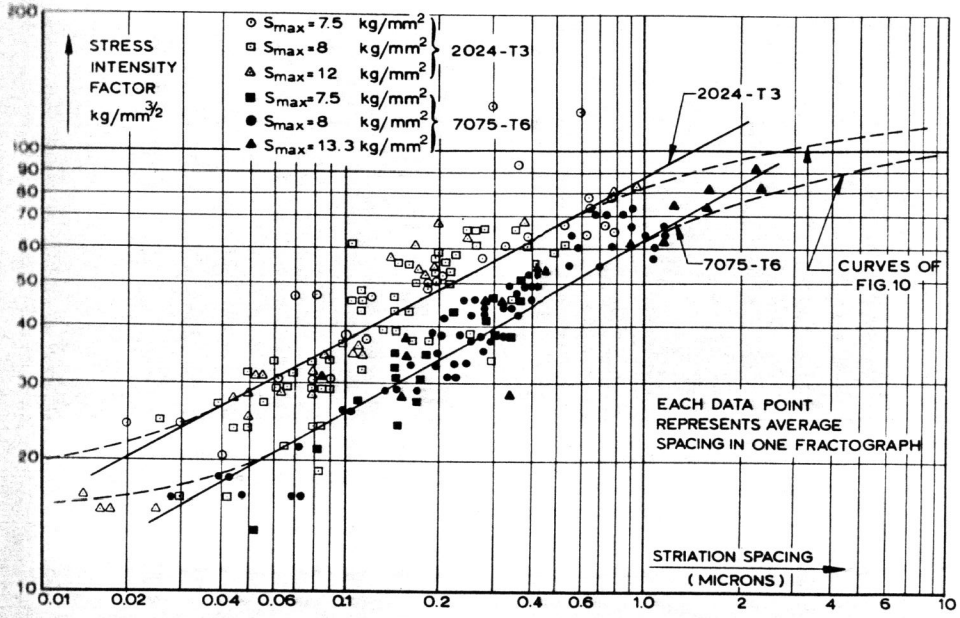

Fig. 11. Relation between stress intensity factor and striation spacing.

Fig. 12. Type I tyre tracks (oblique arrows) in 2024-T3 at low crack growth rate.

Fig. 13. Mechanism of formation of type I tracks according to Beachem.

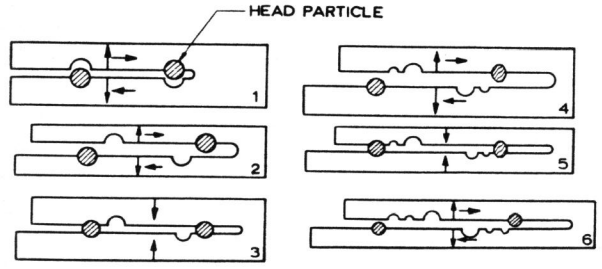

Fig. 14. Type I tyre tracks.

Fig. 15. Type II tyre tracks in 2024-T3 at 100 microns per cycle.

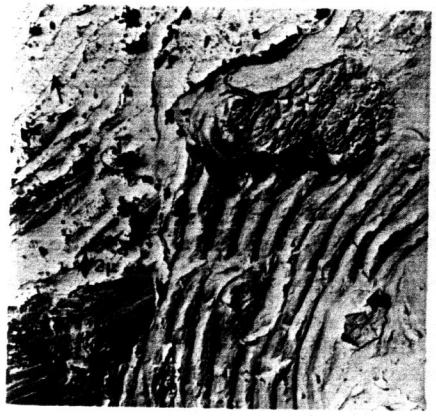

Fig. 16. Type II tyre tracks in 7075-T6 at 10 microns per cycle.

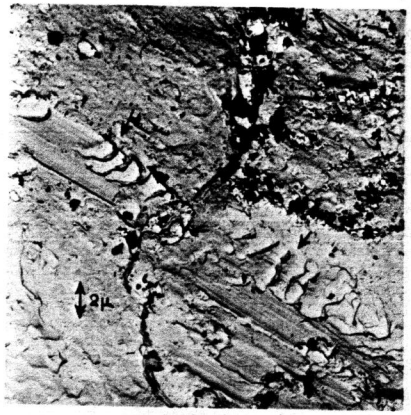

Fig. 17. Mechanism of Type II tyre tracks in 2024-T3.